multi-layer graphene reinforced pure titanium matrix composites by a micro-laminated structure design

Xiaonan Mu[a], Hongnian Cai[a], Hongmei Zhang[a*], Qunbo Fan[a], Yan Wu[a], Suochen Li[a], Yuxin Ge[a]

[a]National Key Laboratory of Science and Technology on Materials under Shock and Impact, School of Materials Science and Engineering, Beijing Institute of Technology, Beijing 100081, China

*Corresponding author: Prof. H.-M. Zhang,

Tel.: +86 10 68913951 605; Fax. : +86 10 6891 3951 608

E-mail address: zhanghm@bit.edu.cn (H. Zhang)

Abstract: In this study, a micro-laminated structure of titanium matrix composite with uniformly dowel-like and aligned multi-layer graphene (MLG) is fabricated by flake powder metallurgy. High energy ball milling method is applied to efficiently obtain flaky Ti powders with embedded MLG flakes. Spark plasma sintering (sps) which can enable the MLG to preserve its original structure. Also, it can consolidate mixed powders to obtain the laminated billet. Subsequent hot-rolling (HR) is applied to control the degree of interfacial reaction and reduce the internal defection of composites. Results show that interface of the composite owns one in-situ formed TiC thin layer between MLG and matrix. Also, the composite with micro-laminated structure shows significant improvement of strength. Consequently, a uniform disperse of only 0.1wt% MLG enables the as-designed composite to exhibit 218% increase of yield strength compared to monolithic matrix.

Keyword: titanium matrix composites; multi-layer graphene; micro-laminated structure; mechanical properties

1. Introduction

MLG is a two-dimensional nanomaterial which has been considered to be one potential new carbon material in the field of material science and engineering due to its remarkable electrical, thermal and mechanical properties [1-3]. In the past decade, MLG have been used to the reinforcement added in polymer and ceramic matrix composites. Rafiee et al. [4] fabricated the epoxy nano-composites with MLG at low content which showed a superiority of modulus and fracture strength compared with pure epoxy. Walker et al. [5] synthesized the high-density MLG/Si_3N_4 with excellent toughness property through SPS method. As for the fabrication of MLG reinforced metal matrix composites, an increasing number of researchers have focused on the fields like aluminum [6-8], magnesium [9], and copper [10-11] matrix materials. A lot of researches have

been found that the MLG offer significant improvement in the mechanical properties, such as tensile strength and wear resistance.

Titanium and titanium alloys have many unique features such as high specific strength and light weight which enhance the potential for the use of Ti as matrix material [12-14]. Titanium matrix composites (TiMCs) can be used in various industries，such as automotive, and airplane industries, to resolve the increasing limited supply of energy resources. Because of the high corrosion resistance, their chemical and petrochemical applications are also excellent. Many researches begin to focus on fabricating MLG reinforced TiMCs due to its potential superior mechanical property compared to conventional TiMCs, such as TiC/Ti, TiB/Ti and SiC/Ti. Shin et al. [15] synthesized 0.7vol% graphene reinforced pure Ti (compressive yield strength ~1.5GPa)by using powder metallurgy. The mixed powders were consolidated by hot-pressing at 570℃ for 1h under 140MPa. Zhen et al. [16] fabricated 0.5wt% MLG/TC4 (by applying hot isostatic pressing (HIP) under 150 MPa at 700℃ followed by isothermal forging with a subsequent forging process at 970℃, specially, the composites exhibit significantly improved strength without losing ductility. X.N. Mu et al. [17] fabricated TiMCs by adding low MLG content (0.025wt%, 0.05wt% and 0.1wt%) by applying sps technique and hot-rolling process, and MLG in matrix exhibit excellent load bearing capacity. In this paper, ball milling method is used to fabricate the flake titanium/MLG mixed powders. The mixed powers are then consolidated by sps and improved by subsequent hot-rolling to obtain novel micro-laminated structure and this architecture enabled the composite display outstanding mechanical properties. The pure Ti is fabricated under the same processing conditions as comparison.

2. Experimental

Ti powders (CPTi, purity>99%) with a mean particle diameter of ~45μm are used as the starting raw material. Table 1 shows characteristics of the Ti powders used in this study. MLG are synthesized from graphene oxides that are prepared by improved Hummers method. Fig. 1(a) shows the scanning electron microscopy (SEM) image of Ti powders. The image shows that the Ti powders with a regular spherical morphology have no aggregation. Fig. 1(b) is the transmission electron microscopy (TEM) image of MLG which shows high aspect ratio and dozens of two-dimensional stacking layers.

The fabrication process of MLG/Ti mainly contains three steps. a) Dispersion, ball milling (BM) method is a relatively more convenient and effective way to mix MLG and metal powders [18]. One group of 30g Ti powders compound with alcoholic solution are mechanical stirred to form the Ti slurries by 20min. MLG powders are ultrasonic dispersed and mixed with Ti slurries.

Then the Ti slurries containing 0.1wt%MLG are stirred 5min and sealed into agate jar with agate milling balls (ball to powder weight ratio was 10:1). The BM time is 2.5h with 400rpm revolution speed. Fig. 1(c) shows the morphology of mixed powders. It presents that the MLG embedded in Ti platelets with a mean size of 1~2μm. b) Preforming. In this step, we expect to form high-density blocks in which MLG have nearly no reduction product with Ti matrix. It relies on SPS technique which can offer much more rapid heating and cooling rate (>500℃/min) and low sintering temperature [19-20].The dried powders are loaded into steel die with internal diameter 25mm and external diameter 55mm. Sps system (Sojitz Machinery Corporation, Tokyo, Japan) is used to consolidate the mixed powders. The vacuum, applied holding compressive pressure and sintering temperature were adjusted to 1pa, 300MPa and 826K, respectively. The size of cylinder billet was Ø25 × 12. c) Forming. Deformation processing is an effective way to disperse carbon nano-materials in metal matrix and eliminate defects [21]. In this study, hot-rolling (60% reduction) temperature was 1223K to finally form the composites.

The microstructure and fracture morphology of the composites are observed by a field emission scanning electron microscope (FSEM, HITACHI S-4800N, Japan). The interface between MLG and Ti matrix is observed by high resolution TEM (HRTEM, Tecnai G20, FEI, Netherlands). The Raman spectroscopy (Renishaw inVia, excitation laser 514 nm) is used to investigate the structure of GNPs. The Ø4×4 cylindrical specimen was cut along with the rolling direction (RD) for compression test. The Instron 5848 Microtester was used to test at least three samples in each MLG/Ti compress property at the room temperature with the strain rate of $1\times10^{-3}s^{-1}$.

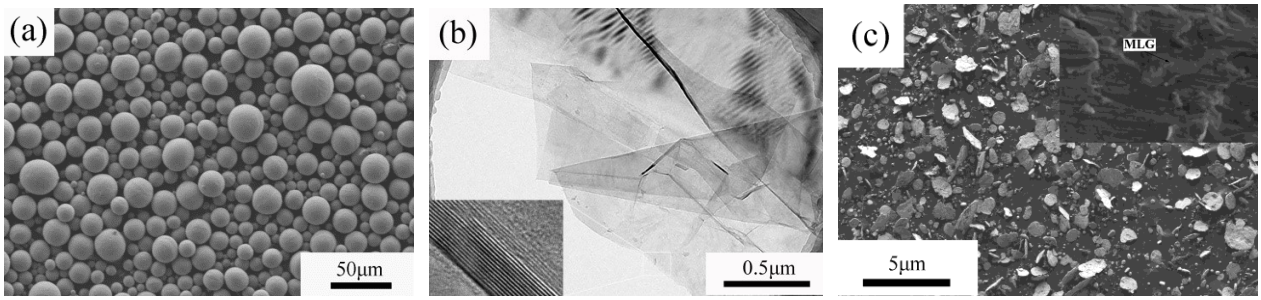

Fig.1 (a) SEM image of pure Ti powders; (b)TEM and HRTEM image of MLG; (c) SEM image of mixed powders.

Table 1

Characteristics of the Ti matrix powders.

Powder	Impurity content (mass%)					Ture density (g/cm^3)	Bulk density (g/cm^3)	Particle size (μm)
CPTi	O	Fe	N	C	H			
	0.15	0.07	0.01	0.01	0.003	4.51	1.25	~45

3. Results and discussion

Fig. 2 shows the SEM microstructure of the rolled composites and pure Ti (transverse cross-section). The pure Ti flake powders are sintered and hot rolled under the same processing conditions. It can be seen strong texture along with the rolling direction (RD) shown in Fig. 2(a). Fig. 2(b) shows the SEM microstructure of 0.1wt%MLG/Ti billet. It can be observed that Ti and MLG flakes compactly accumulate with each other to form a laminated structure due to the high pressure of sps. Moreover, some MLG cluster (indicated by white circles) still exist on the boundary because of the limited nano-dispersion capability of ball milling method [17].Although the high chemical reactivity about to the C and Ti, the reaction between MLG and Ti matrix can be neglected during sps process [14]. Fig. 2(c) shows the SEM microstructure of HR 0.1wt%MLG/Ti composite. It confirms that MLG are dispersed homogeneously under 1223K HR. The HR process effectively prevents the negative influence of MLG agglomerations and defects on the properties of MLG/Ti composites. MLG with a size of 1-2μm embeds in the matrix of the sample. The grain size of the Ti matrix is smaller than the raw Ti flakes with the adding of MLG. Higher magnification (shown in Fig. 2(d)) image of HR 0.1wt%MLG/Ti composite indicated that the MLG preserved its original structure attributed to the rapid HR process. Furthermore, some MLG flakes insert into the Ti grain boundary with angle of 30° ~60° (indicated by blue circles), the other MLG flakes with small angle of 0° ~15° nearly flat on the Ti grain boundary (indicated by yellow circles). It is hypothesized that the formation of this special laminated structure origin to the ball milling process (shown in Fig. 3).During ball milling, flaky Ti is gradually produced under the impact between high-energy balls (ZrO_2, 1cm). Simultaneously, dispersed MLG flakes in alcohol solution are impacted on flaky Ti powders. Attribute to the strong mechanical impact, MLG flakes are strongly attached on the surface of Ti flaky powders with a fully MLG-Ti contact (flat on the surface) and partly MLG-Ti contact (insert into powders).

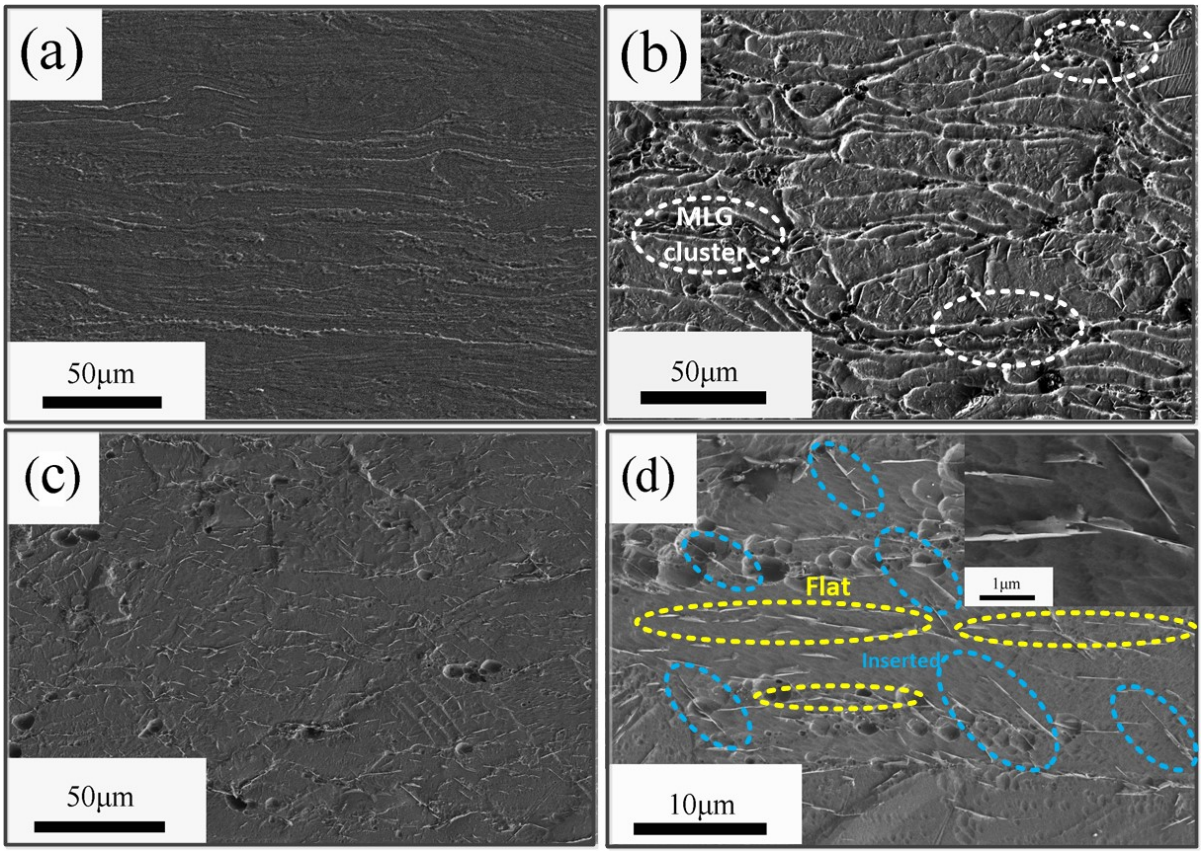

Fig.2 SEM micrographs of MLG/Ti (a) HR pure Ti (b) sintered MLG/Ti billet (c-d) HR MLG/Ti composite

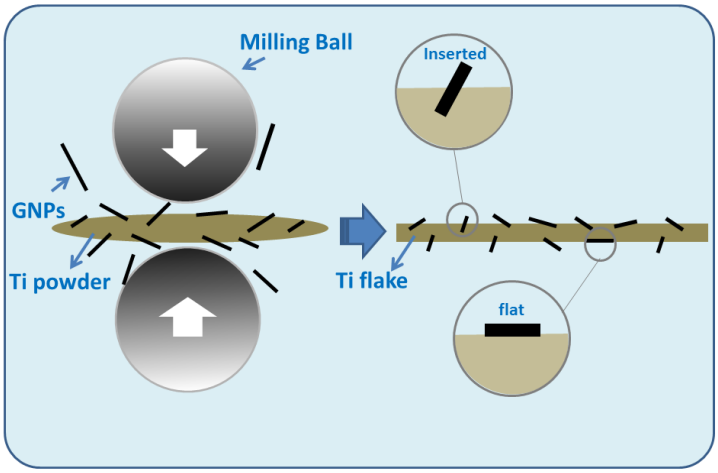

Fig. 3 Scheme of ball milling process for MLG dispersion

Fig. 4(a) presents the Raman spectra of the raw MLG and the HR 0.1wt%MLG/Ti composites. It can be seen that the two materials reveal the presence of D peaks (from defect and amorphous carbon), G peaks (from graphite) and 2D peaks (shape of the second-order Raman bands) in the positions [22-24]. The relative density between D and G peaks (I_D/I_G) indicated the structural defects and domain size in graphitic materials [25-26].The I_D/I_G ratio increases significantly (from

0.2 to 0.6) after HR process. It is indicated that the introduction of disorder and defects to MLG structure exist during HR. The ratio between the intensities of the 2D and G peaks, I_{2D}/I_G, is about 4 for singer layer graphene and decrease with an increase of stacking-layer number of MLG [27]. Also, the 2D peaks will become narrower and sharper when the thickness of MLG decreases [28]. In this study, the raw MLG powders and HR 0.1wt%MLG/Ti composites exhibit the ratio of 2D and G peaks far less than 4, thus indicated that the MLG structure is conserved in matrix during HR process. The increase of I_{2D}/I_G ratio from 0.4 to 0.5 presented that the stacking-layer number of MLG is reduced due to sps and HR process. Moreover, the Raman results can be proved by Fig. 4(b). Amount of defects may form due to the formation of TiC (reaction diffusion) layer between MLG and matrix. Since the surface layer of the MLG offer the C atoms to react with Ti matrix, thus the original structure of MLG may destroyed through reaction. Moreover, the stacking layer of the MLG will also be reduced with reaction continues. It is worth mentioning that the MLG can exhibit efficient load bearing ability due to the firm and clear interface, thus may provide great improvement of mechanical property for the composite.

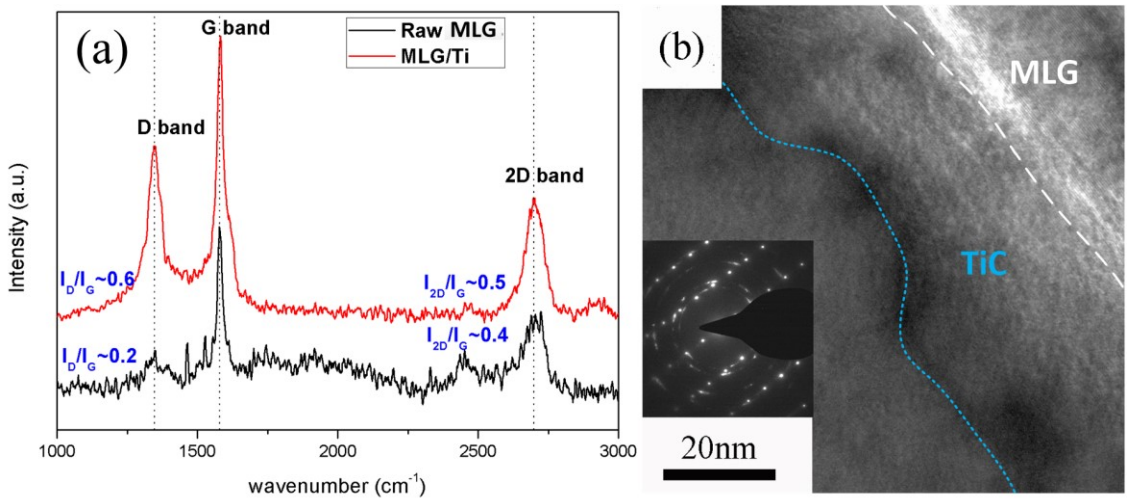

Fig. 4 (a) Raman spectra of raw MLG powders and HR 0.1wt%MLG/Ti composites (b) HRTEM of HR 0.1wt%MLG/Ti composites

Fig. 5(a) shows the compression strain-stress curves of pure Ti and HR 0.1wt%MLG/Ti composites. The strength of MLG/Ti is significantly increased in relative to that of the monolithic pure Ti. The yield strength (σ_s) is increased to 1540MPa from 485MPa, or by 218% increment compared with that of pure Ti. The fracture strength of MLG/Ti is about 2.3GPa when the plastic deformation is 32% (fracture strain), and nearly 2 times higher than that of pure Ti in the same strain value. The moderate ductility is believed to be relative to the interpenetrating Ti matrix phase, and the dowel-like structure of strong MLG. Fig. 5(b) shows schematic illustrations of the features

of distribution of MLG reinforcement. MLG links the adjacent flaky Ti grains like dowel connector. In addition, SEM microstructure (shown in Fig. 5(a)) shows that the MLG distributes on the failure surface. In order to analyze the fracture mode of MLG when the composite is loaded, the critical length (l_c) of MLG can be defined as [29]:

$$l_c = \sigma_\gamma \frac{Al}{\tau_m S} \quad (1)$$

where σ_γ is yield stress of the MLG (~30GPa), A and l are cross-section areas and length of MLG respectively, S is interfacial areas. , τ_m is the shear strength of titanium matrix ($\approx 0.5\sigma_m$, σ_m is the yield strength of matrix). The calculated l_c for MLG/Ti composite is about 3.6μm, which is larger than the average MLG size (1~2μm). This means that the stress on the MLG impossibly reach to the fracture strength of the MLG. Thus, the MLG on the fracture surface might be directly pull out from the Ti matrix。

The strength increase of MLG/Ti composite is thought to be contributed from a combination of effective load bearing effect, grain refinement, Orowan looping and texture strengthening mechanism. In this work, the in-situ formed TiC layer around the interface between MLG and matrix could be a reinforcement and trend to drastically strengthen the interface. Thus the load bearing effect may attribute to the combination effect of MLG and TiC layer. It should be noticed that the Ti grain size is obviously refined due to the MLG uniformly dispersed into matrix, thus the grain refinement is an important reason for the strength increase. Orowan looping is another main strengthening mechanism for ultrafine particle/composite, the formation of residual dislocation loops around by MLG which produces a back stress that prevent the motion of dislocation leading to an increase in the yield stress ($\Delta\delta_{OR}$). The $\Delta\delta_{OR}$ can be expressed as follows [30]:

$$\Delta\sigma_{OR} = \frac{0.13Gb}{d_p[(\frac{1}{2V_{GNPs}})^{\frac{1}{3}}-1]} \ln(\frac{d_p}{2b}) \quad (2)$$

where b is Burger vector of matrix, d_p is the average particle size of mlg, G is the shear modulus of titanium. In our previous work [17], [0001] texture in composites matrix parallel to RD and become stronger than in pure Ti due to hot-rolling process. During compressive deformation, the conventional slip system <11$\bar{2}$0> (0002) in composites normal to compressive axis is hard to rotate in matrix. Thus, the texture strengthening mechanism is also an important factor which contributes to the strength improvement of composite.

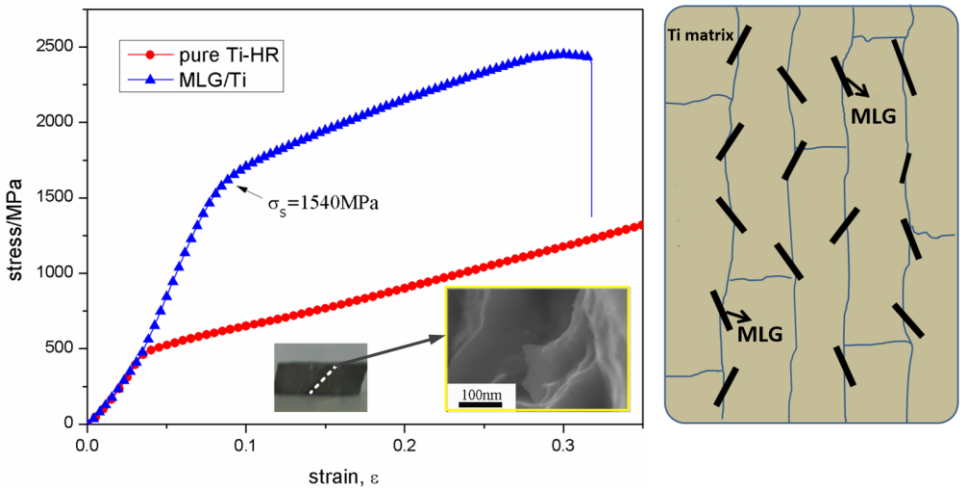

Fig. 5 (a) Engineering strain-stress curves of pure Ti and HR 0.1wt% MLG/Ti composites (b) Distribution of reinforcements and dowel structure of MLG

4. Conclusions

High energy ball milling with subsequent sps and HR process is successfully used to fabricate 0.1wt% MLG/Ti composites with uniformly dispersed MLG. The composite owns novel micro-laminated structure with dowel-like and aligned MLG. The MLG-Ti interfaces are well bonded through one newly in-situ formed TiC layer and the original structure of MLG is retained. The strength of MLG/Ti composite is significantly higher than that of the matrix pure Ti. In particular, the 0.1wt% MLG/Ti composite exhibits an yield strength of 1530MPa along with a relatively high failure strain. This paper highlights the advantages of new designed micro-laminated composites that introduce MLG into Ti matrix as one two-dimensional carbon reinforcement because of their outstanding potential to strengthen TiMCs.

Acknowledgments

The supports from the Research Foundation of National Key Laboratory of Science and Technology (Grant no. 61429020106162902001) on Materials under Shock and Impact is gratefully acknowledged.

References

[1] A.K. Geim, K.S. Novoselov. The rise of graphene. *Nature materials* 6(2007):183–191.

[2] S. Park, R.S. Ruoff, Chemical methods for the production of graphenes. *Nature Nanotechnology* 5(2010):217–224.

[3] K.S. Novoselov, A.K. Geim, S.V. Morozov, D. Jiang, Y. Zhang, S.V. Dubonos, I.V. Grigorieva, A.A.

Firsov. Electric field effect in atomically thin carbon films. *Science.* 306(2004):666–669.

[4] M.A. Rafiee, J. Rafiee, Z. Wang, H. Song, Z.Z. Yu, N. Koratkar, Enhanced mechanical properties of nanocomposites at low graphene content. *Acs Nano*. 3 (2009): 3884-3890.

[5] L.S. Walker, V.R. Marotto, M.A. Rafiee, N. Koratkar, E.L. Corral, Toughening in graphene ceramic composites. *Acs Nano*. 5 (2011):3182-3190.

[6] M. Rashad, F.S. Pan, A.T. Tang, M. Asif, Effect of Graphene Nanoplatelets addition on mechanical properties of pure aluminum using a semi-powder method. *Prog. Nat. Sci*. 24 (2014): 101–108.

[7] R. Pérez-Bustamante, D. Bolaños-Morales, J. Bonilla-Martínez，I. Estrada-Guel，R. Martínez-Sánchez, Microstructural and hardness behavior of graphene-nanoplatelets/aluminum composites synthesized by mechanical alloying. *J. Alloys Comp.* 615 (2014) S578–S582.

[8] J.Y. Wang, Z.Q. Li, G.L. Fan, H.H. Pan, Z.X. Chen, D. Zhang, Reinforcement with graphene nanosheets in aluminum matrix composites. *Scr. Mater.* 66 (2012): 594–597.

[9] M. Rashad, F.S. Pan, A.T. Tang, M. Asif, M. Aamir, Synergetic effect of graphene nanoplatelets (GNPs) and multi-walled carbon nanotube (MW-CNTs) on mechanical properties of pure magnesium. *J. Alloys Comp*. 603 (2014):111–118.

[10] F.Y. Chen, J.M. Ying, Y.F. Wang, S.Y. Du, Z.P. Liu, Q. Huang, Effects of graphene content on the microstructure and properties of copper matrix composites. *Carbon.* 96 (2016):836-842.

[11] D. Zhang, Z.J. Zhan, Preparation of graphene nanoplatelets-copper composites by a modified semi-powder method and their mechanical properties. *J. Alloys Comp.* 658 (2016): 663-671.

[12] K. Kondoh, T. Threrujirapapong, J. Umeda, B. Fugetsu, High-temperature properties of extruded titanium composites fabricated from carbon nanotubes coated titanium powder by spark plasma sintering and hot extrusion. *Composites science and technology* 72 (2012):1291–1297.

[13] S.C. Tjiong, Y.W. Mai, Processing-structure-property aspects of particulate- and whisker-reinforced titanium matrix composites. *Composites science and technology* 68 (2008): 583-601

[14] F.C. Wang, Z.H. Zhang, Y.J. Sun, Y. Liu, Z.Y. Hu, H. Wang, A.V. Korznikov, E. Korznikova, Z.F. Liu, S. Osamu. Rapid and low temperature spark plasma sintering synthesis of novel carbon nanotube reinforced titanium matrix composites. *Carbon.* 95(2015): 396-407.

[15]S.E. Shin, H.J. Choi, J.Y. Hwang, D.H. Bae, Strengthening behavior of carbon/metal nanocomposites. *Sci. Rep.* 5 (2015): 1-7.

[16] Zhen Cao, Xudong Wang, Jiongli Li, et al. Reinforcement with graphene nanoflakes in titanium matrix composites. *J. Alloys Comp.* 696 (2017): 498-502.

[17] X. N. Mu, H. M. Zhang, H. N. Cai, Q. B. Fan，Z. H. Zhang, Z. J. Fu, D. H. Yu. Microstructure evolution and superior tensile properties of low content graphene nanoplatelets reinforced pure Ti matrix composites. *Materials Science & Engineering A*. 687 (2017):164-174.

[18]W.J. Kim, T. J. Lee, S.H. Han. Multi-layer graphene/copper composites: Preparation using high-ratio differential speed rolling, microstructure and mechanical properties. *Carbon* 69 (2014):55-65

[19] A. Nieto, D. Lahiri, A. Agarwal, Synthesis and properties of bulk graphene nanoplatelets consolidated by spark plasma sintering, *Carbon*. 50 (2012):4068-4077.

[20] Z.H. Zhang, Z.F. Liu, J.F. Lu, X.B. Shen, F.C. Wang, Y.D. Wang, The sintering mechanism in spark plasma sintering - proof of the occurrence of spark discharge. Scripta Mater. 81 (2014) 56-59.

[21] I. Barin, O. Knacke, O. Kubaschewski O, Thermao chemicalproperties of inorganic substance. 2nd ed. NewYork: Springer-Verlag; 1991.

[22] C. Castiglioni, M. Tommasini, G. Zerbi. Raman spectroscopy of polyconjugated molecules and materials: confinement effect in one and two dimensions. *Phil Trans R Soc Lond A*. 362 (2004): 2425–2459.

[23] Dresselhaus MS, Jorio A, Hofmann M, Dresselhaus G, Saito R. Perspectives on carbon nanotubes and graphene Raman spectroscopy. *Nano Lett* 10 (2010): 751–758.

[24] K. N. Kudin, B. Ozbas, H. C. Schniepp, R. K. Prud'homme, I. A. Aksay, R. Car. Raman spectra of graphite oxide and functionalized graphene sheets. *Nano Lett* 8 (2008):36–41.

[25] E. F. Antunes, A. O. Lobo, E. J. Corat, V. J. Trava-Airoldi, A. A. Martin, C. Verı´ssimo. Comparative study of first- and second-order Raman spectra of MWCNT at visible and infrared laser excitation. *Carbon* 44(2006):2202–2211.

[26] C. He, N. Q. Zhao, C. S. Shi, X. W. Du, J. J. Li, H. P. Li, et al. An approach to obtaining homogeneously dispersed carbon nanotubes in Al powders for preparing reinforced Al–matrix composites. *Adv Mater* 19 (2007):1128–1132.

[27] X. N. Mu, H. M. Zhang, H. N. Cai, Q. B. Fan, Z. H. Zhang, Z. J. Fu, D. H. Yu. Microstructure evolution and superior tensile properties of low content graphene nanoplatelets reinforced pure Ti matrix composites. *Materials Science & Engineering A*, 687 (2017):164-174.

[28] D. Li, D. Zhan, J. Yan, C. L. Sun, Z. W. Li, Z. H. Ni, et al. Thickness and stacking geometry effects on high frequency overtone and combination Raman modes of graphene. *J Raman Spectrosc* 44 (2013):86–91.

[29] S.E. Shin, H.J. Choi, J.H. Shin, D.H. Bae, Strengthening behavior of few-layered graphene/aluminum composites, *Carbon.* 82 (2015) 143–151.

[30] Z. Zhang, D.L.Chen, Consideration of Orowan strengthening effect in particulate-reinforced metal matrix nanocomposites: A model for predicting their yield strength. *Scr. Mater.* 54 (2006):1321–1326.